Supporting Information

Insight into the Effect of Water on the Methanol-to-Olefins Conversion in H-SAPO-34 from Molecular Simulations and in Situ Microspectroscopy

Kristof De Wispelaere,[a,c] Caterina S. Wondergem,[b] Bernd Ensing,[c] Karen Hemelsoet,[a] Evert Jan Meijer,[c] Bert M. Weckhuysen,[b]* Veronique Van Speybroeck [a]* and Javier Ruiz-Martínez [b]**

[a] Center for Molecular Modeling (CMM), Ghent University, Technologiepark 903, 9052, Zwijnaarde, Belgium

[b] Inorganic Chemistry and Catalysis, Debye Institute for Nanomaterials Science, Utrecht University, Universiteitsweg 99, 3584 CG, Utrecht, The Netherlands

[c] Amsterdam Center for Multiscale Modeling and van 't Hoff Institute for Molecular Sciences, University of Amsterdam, Science Park 904, 1098 XH Amsterdam, The Netherlands

*Corresponding authors: E.J.Meijer@uva.nl, B.M.Weckhuysen@uu.nl, Veronique.VanSpeybroeck@ugent.be, J.RuizMartinez@uu.nl

Contents

S1. Additional computational details

Except for the $(1:1)_{mw,sim}$ (see section S3) mixture, all simulations were performed with a H-SAPO-34 unit cell containing two acid sites, located in the same 8-ring as shown in Figure S1. This corresponds to a catalyst with (Al+P)/Si ratio of 17. As already mentioned, the simulation on the competition between one water and methanol molecule for direct interaction with the BAS ($(1:1)_{mw,sim}$ composition) was performed in a unit cell containing only one BAS to simplify the interpretation of the results. Hereby, the cell volume of the simulation with 1 methanol molecule was used for the NVT run.

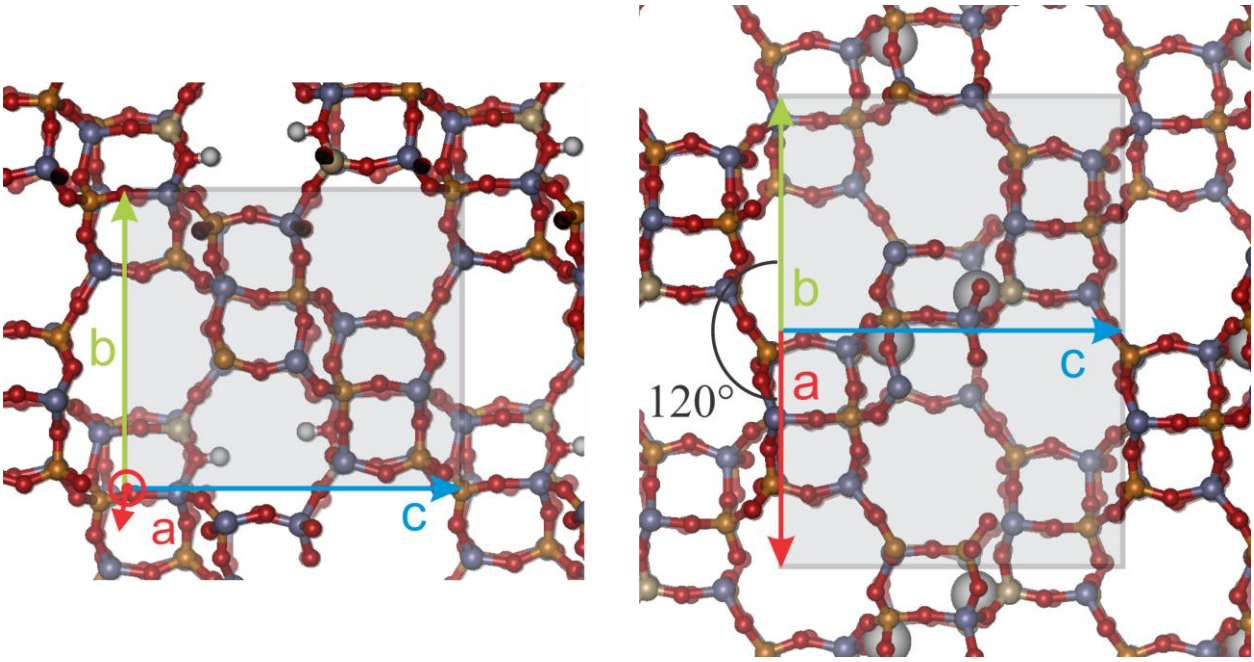

Figure S1. H-SAPO-34 unit cell (shaded area) containing two acid sites.

During the experiments, H-SAPO-34 crystals with a (Al+P)/Si ratio of 4.9 were used. We would like to stress that in the simulations we only look at local effects occurring in the neighborhood of an 8-ring containing one or more BASs connecting two CHA cages. To simplify the models

we therefore opted to limit the number of BASs to two, located in one 8-ring as shown in the central panel of Figure S2. However, additional simulations have been performed for high loadings of methanol ($(5:0)_{mw,sim}$ with 1 BAS and 4 BASs per unit cell (left and right panel in Figure S2). A major difference between these simulations is the probability that the framework deprotonates (denoted as FDP in the manuscript). These probabilities range from 100 % for 1 and 2 BAS to 63 % for 4 BASs when 10 methanol molecules are adsorbed per unit cell. This is of course due to the lower methanol concentration per BAS with an increased number of BAS. It thus seems that the absolute numbers shown in Figure 1a of the manuscript depend on the acid site density. However, as mentioned in the manuscript, the competition between methanol and water for access to the acid site has been observed for 1 BAS and 2 BAS per unit cell. It can indeed be expected that this competitive behavior is not severely influenced by the acid site density. As our major conclusions are based on this competitive effect rather than on the exact probabilities that framework deprotonation occurs, we can state that the discrepancy between the acid site densities in simulations and experiments do not alter the conclusions of this paper.

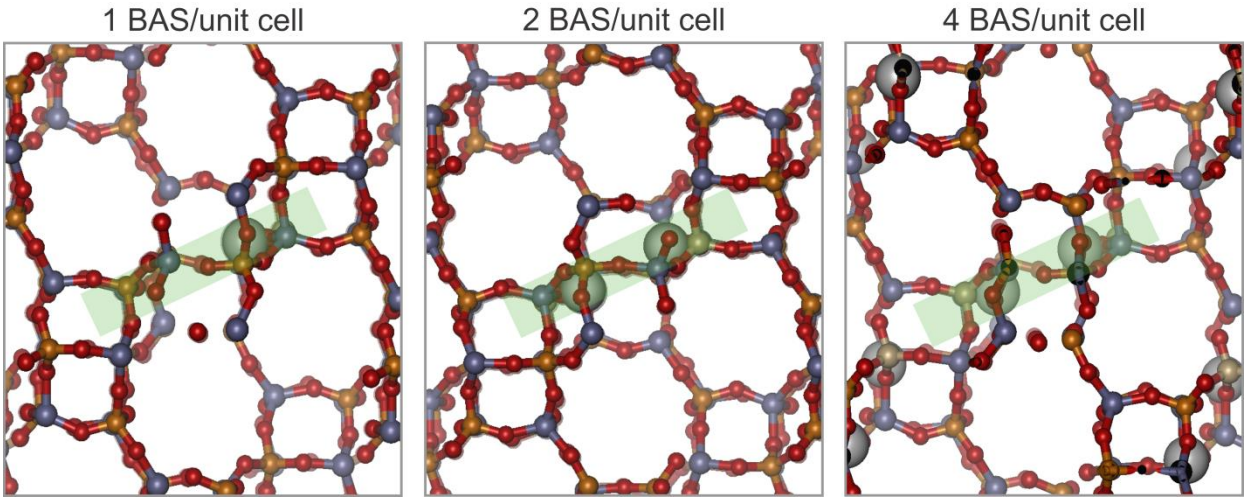

Figure S2. Unit cell of H-SAPO-34 containing 1 BAS (left), 2 BAS (middle) and 4 BAS (right). The green area highlights the position of the 8-ring containing one or more BAS.

Optimized unit cell volumes

NPT molecular dynamics (MD) simulations were performed at 350 ºC and 1 bar. After an equilibration run of 5 ps, a production run of 50 ps is performed. Hereby, the zeolitic framework is fully flexible. The temperature is controlled via a chain of 5 Nosé-Hoover thermostats. An integration time step of 0.5 fs was applied. The appropriate cell parameters were obtained from the NPT MD simulations with the appropriate guest molecules adsorbed in the framework and are summarized in Table S1.

Table S1. Average cell parameters of the H-SAPO-34 unit cell containing 2 acid sites obtained after NPT simulations at 330ºC and 1 bar with different loadings of methanol and water.

$(x:y)_{mw,sim}$	V (Å^3)	a (Å)	b (Å)	c (Å)	α (º)	β (º)	γ (º)
$(1:0)_{mw,sim}$	2553.93	14.07	14.10	14.87	90	90	120
$(0:1)_{mw,sim}$	2545.59	14.09	14.13	14.76	90	90	120
$(5:0)_{mw,sim}$	2584.06	14.02	14.09	15.10	90	90	120
$(2:2)_{mw,sim}$	2575.41	14.03	14.10	15.03	90	90	120
$(1:4)_{mw,sim}$	2555.32	14.01	14.09	14.95	90	90	120
$(1:8)_{mw,sim}$	2575.42	14.04	14.05	15.07	90	90	120

Framework deprotonation and methanol protonation

The probabilities of framework deprotonation (FDP) and methanol protonation (MP) were calculated based on a geometrical analysis of the MD trajectories. The framework was considered as deprotonated if for at least one of the two acid sites in the unit cell the shortest proton-O_z distance exceeded 1.2 Å, with O_z one of the oxygen atoms surrounding the substitutional defect. Methanol and water were considered to be protonated if the shortest proton-

oxygen distance was less than 1.3 Å. The cut-off values were chosen such that the following equality is valid with a tolerance of 2%:

$$P(FDP) \approx P(MP) + P(WP),$$

where P(FDP), P(MP) and P(WP) are the probabilities for framework deprotonation, methanol protonation and water protonation, respectively.

Metadynamics

The reported metadynamics simulations were carried out at 330 °C in the NVT ensemble, using the time-averaged cell parameters from the NPT runs. The temperature during the simulations is controlled by a chain of 5 Nosé-Hoover thermostats. The metadynamics method has been developed by Laio and Parrinello,[1-5] and is very promising to study zeolite-catalyzed reactions as was earlier demonstrated by some of the present authors.[6-9] The method relies on the choice of a limited number of collective variables along which the free energy landscape is "filled up" with Gaussian-shaped bias potentials to accelerate sampling of rare events (Figure S3). Afterwards the sum of the Gaussians can be used to reconstruct the free energy surface (FES). The method is especially suited to explore new reaction pathways by identifying a set of collective variables that allow sampling interesting regions of the potential energy surface. For the simulation of chemical reactions, it is especially useful to use coordination numbers.

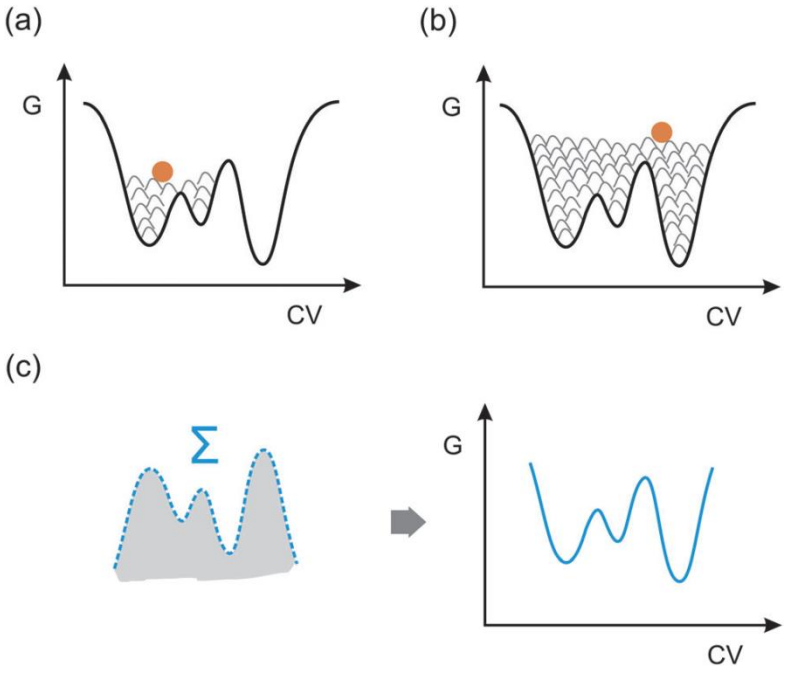

Figure S3. Schematic representation of the metadynamics approach. Free energy minima are "filled" with Gaussian-shaped bias potentials or hills (a), when all minima and all transitions are sampled (b), the inverse of the sum of all Gaussians yields a reconstruction of the sampled free energy surface (c). Reproduced with permission from ref. 10. Copyright 2014 The Royal Society of Chemistry.

During the MTD simulations, Gaussian hills are spawned along two collective variables (CV), defined by coordination numbers (CN):

$$CN = \sum_{i,j} \frac{1-(r_{ij}/r_0)^{nn}}{1-(r_{ij}/r_0)^{nd}}$$

where the sum runs over two sets of atoms *i* and *j*, r_{ij} is the distance between atoms *i* and *j* and r_0 is a reference distance. For all coordination numbers used in this study, a reference distance r_0 of 1.59 Å was chosen. The parameters *nn* and *nd* are set to 6 and 12, respectively.

Quadratic walls were used to restrict the exploration of the FES to a particular area of interest. The reacting methanol molecule is kept close to the acidic proton and the product valley is not entirely sampled to enhance barrier recrossings. After the first and second re-crossing of the transition point, the hill height is adequately halved. Hills with heights of 5 kJ/mol – 2.5 kJ/mol – 1.25 kJ/mol and 0.625 kJ/mol were used. A new hill was spawned every 50 time steps. The width of the Gaussians was set to 0.02 for CV1 and 0.008 for CV2. The integration time step was set to 0.5 fs for all MTD simulations.

Walls

Simulation with 5 MeOH / acid site:

- $0.01 \leq CN1$ with K = 100.0 hartree
- $0.04 \leq CN2 \leq 0.4$ with K = 1000.0 and 10.0 hartree

Simulation with 1 MeOH + $4H_2O$ / acid site:

- $0.01 \leq CN1$ with K = 100.0 hartree
- $0.008 \leq CN2 \leq 0.4$ with K = 1000.0 and 10.0 hartree

The total simulation time for the methoxide formation simulations in the $(1{:}0)_{mw,sim}$ and $(5{:}0)_{mw,sim}$ compositions were 180 and 50 ps, during which 7199 and 1999 hills were spawned, respectively. For the $(1{:}4)_{mw,sim}$ mixture, the simulation time was 30 ps, during which 1199 hills were spawned.

S2. Additional experimental details

In-situ cell design

The cell was made of stainless steel; see a picture and schematic representation in Figure S4. The cell was made of metal to avoid previous issues due to the refraction of the light in glass cells. This design featured an air tight lid which could easily be unscrewed prior to and after every experiment. The window in the lid could also be changed so a quartz window could be used for UV-Vis micro-spectroscopy and confocal fluorescence microscopy experiments. The cell is equipped with a thermocouple allowing an adequate monitoring of the temperature during all experiments. The gas connections were also adjusted with a 1/8 stainless steel Swagelok tube with bolts. The cell was fixed into the Linkam cell adequately in order to make it stable for the microscopy experiments.

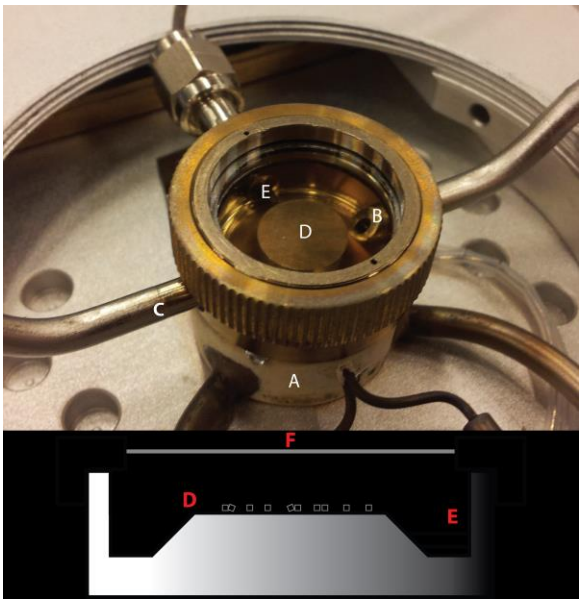

Figure S4. Photograph of the custom-made in-situ cell enclosing a A) heating element of a Linkam Cell, B) inlet gases, C) outlet gases, D) sample holder, E) thermocouple and F) a 0.2 mm quartz lid.

UV-Vis micro-spectroscopy measurements

The UV-Vis micro-spectroscopy set-up is illustrated in Figure S5. The H-SAPO-34 crystals were placed in an in-situ cell using the tip of a Pasteur pipette. A lid with a 0.2 mm quartz window (transparency of 98 % between 200 nm and 2000 nm [11]) was used as a transparent element to seal the cell. After proper sealing, the cell was placed in the heating stage of a Linkam Cell and then was installed underneath an Olympus BX41M microscope connected to an Avantes AvaSpec-2048TEC UV-Vis spectrometer. The samples were illuminated with a 75 W tungsten lamp. The microscope set-up was equipped with a 50/50 double-viewport tube, which accommodate a charge-coupled device (CCD) video camera (ColorView IIIu, Soft Imaging System GmbH) and an optical fibre mount. The microscope was connected to a CCD UV-Vis spectrometer (AvaSpec-2048TEC, Avantes) by a 200-mm-core fibre. Spectra were recorded in absorbance mode and saved automatically every 5 s from the moment that methanol was introduced into the system; this was defined as the start of the experiment. The integration time and average for each spectrum were 50 ms and 100, respectively. The detection range was 390-751 nm. Spectra were recorded in the middle of a crystal and with a spot size of 2 μm. The H-SAPO-34 crystals were used as white reference and a black reference was obtained by shuttering the UV-Vis spectrometer.

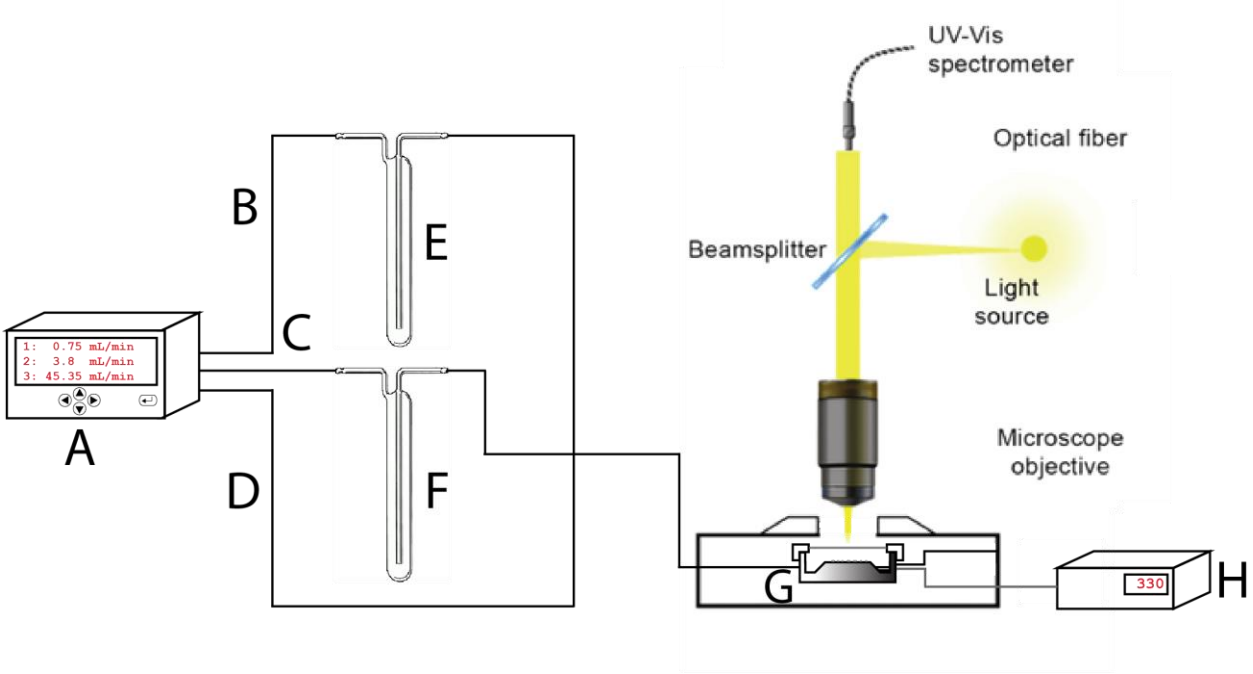

Figure S5. Schematic representation of the UV-Vis micro-spectroscopy set-up. A: Mass flow controller box. B: N_2;MeOH line. C: N_2;H_2O line. D: N_2 line. E: Methanol saturator. F: Water saturator. G: In situ cell. H: Thermocouple read out box.

Confocal fluorescence microscopy experiments

The confocal fluorescence microscopy measurements were performed with the same in-situ cell and experimental protocol as compare to the UV-Vis microscopy measurements. Confocal fluorescence experiments were performed using a Nikon Eclipse 90i upright microscope with a 50x0.55 NA dry objective lens.

S3. Dynamical assessment of methanol and water adsorption in H-SAPO-34

Figure S6 displays the probability density of the distance between the methanol or water molecules in the system and the acid sites. Note that the two curves in Figure S6 correspond to two different methanol or water molecules in the system, as the unit cell containing two acid sites is loaded with one protic molecule per acid site. Apparently, also conformations in which methanol or water do not directly interact with the BAS are sampled, which can be attributed to the relatively high temperature of 330 °C. When taking the time-average of the potential energies of such simulations, the calculated adsorption enthalpies will be lower compared to calculated values at the minimal temperature (-273 °C) due to this thermal effect.

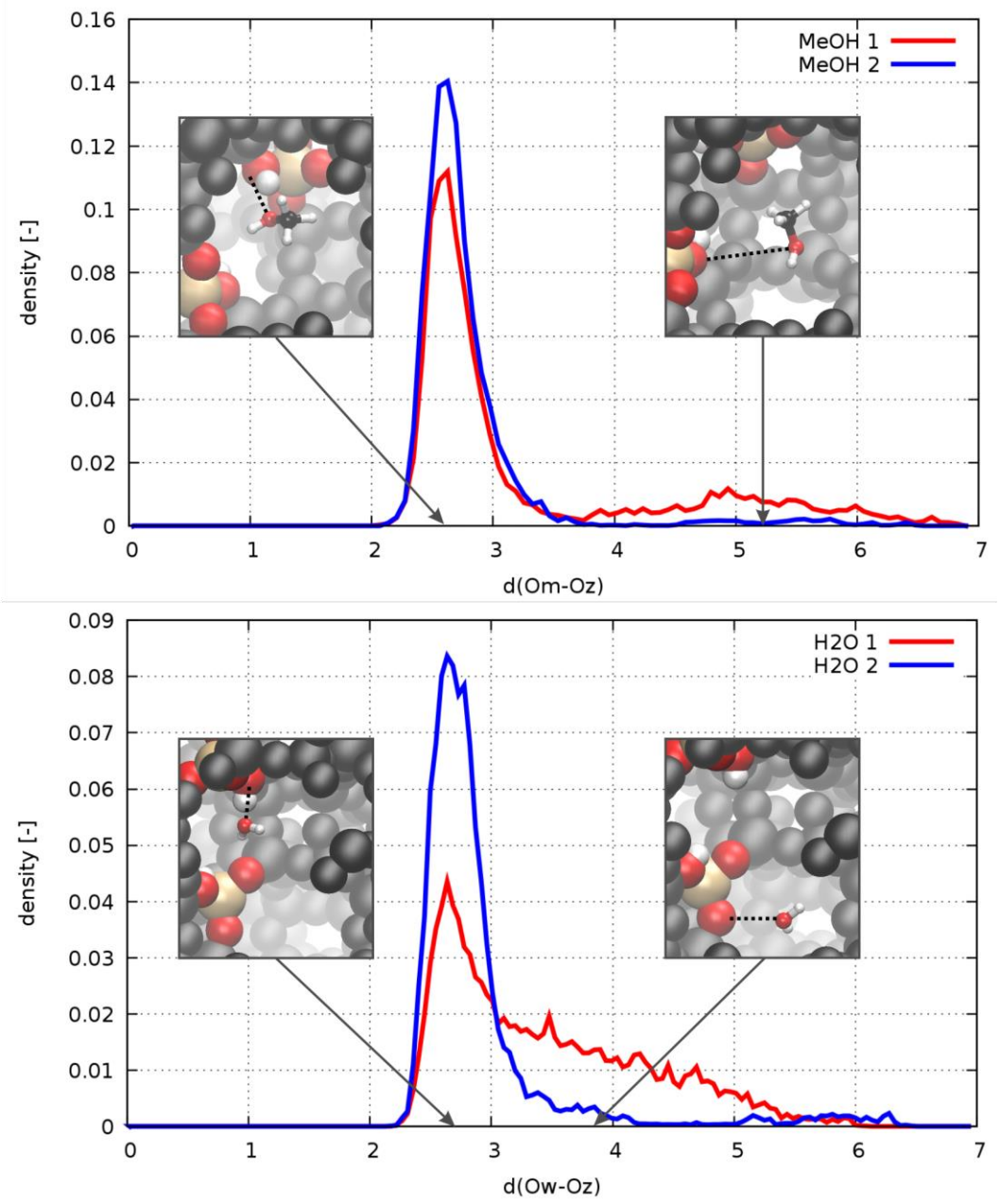

Figure S6. Probability density of the distance of methanol (top) or water (bottom) to the acid sites (highlighted in the insets) during an MD simulation of H-SAPO-34 loaded with 1 methanol or 1 water molecule per acid site, i.e. the $(1:0)_{mw,sim}$ and $(0:1)_{mw,sim}$ compositions from Scheme 2, at 330 °C and 1 bar.

The $d(O_m\text{-}O_z)$ and $d(O_w\text{-}O_z)$ distances shown in Figure S6 correspond to the shortest distance between the methanol or water oxygen atom and a framework oxygen surrounding the substitutional defect.

The competition between water and methanol to form a hydrogen bond with the BAS in H-SAPO-34 was explicitly studied with an MD simulation at 330 °C. To this end, a unit cell was constructed containing only one BAS, one water and one methanol molecule (Figure S7). Although removing an acid site from the unit cell may change the acid strength of the BAS, we opted to perform this simulation with only one acid site to simplify the interpretation of the results. Water and methanol were considered as directly interacting with the BAS if the distance between their oxygen atom and the closest framework oxygen surrounding the substitutional defect was lower than 3.5 Å. A nearly equal probability of water and methanol directly interacting with the BAS was observed, which indicates that water and methanol are indeed able to compete for the BAS (Figure S8). This competition of water with oxygenates and hydrocarbons for acid sites was already suggested in the early 1990s by Marchi and Froment after their experiments on the MTO reaction in H-SAPO-34 with a water containing feed.[12]

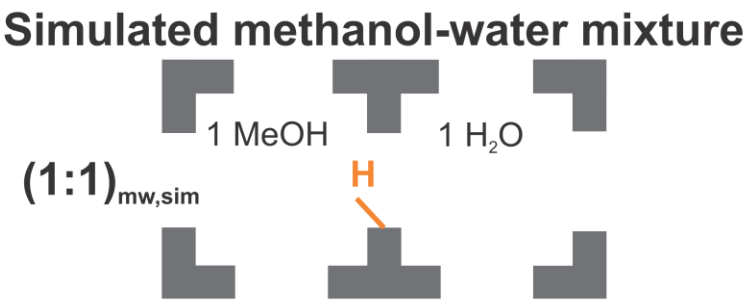

Figure S7. Simulation cell for a $(1:1)_{mw,sim}$ methanol-water mixture. Note that the unit cell contains only one acid site.

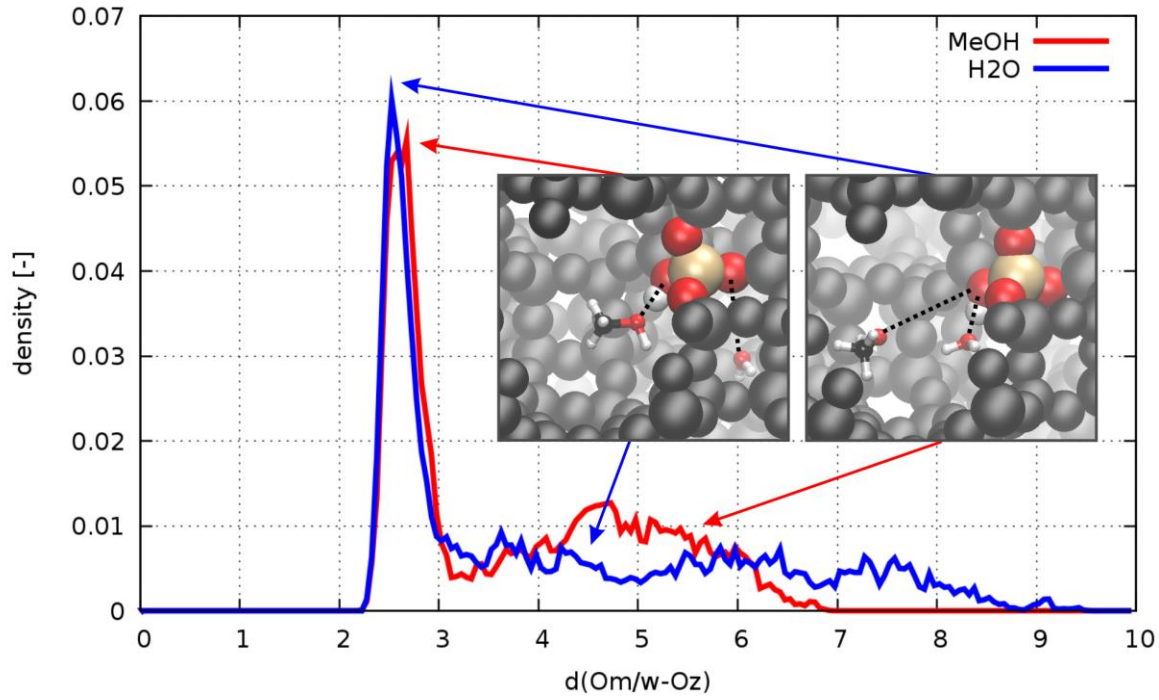

Figure S8. Probability density of the distance of methanol and water to the acid sites during an MD simulation of H-SAPO-34 loaded with 1 water and 1 methanol molecule per acid site ($(1:1)_{mw,sim}$) at 330 °C. In the snapshots the acid site is highlighted.

S4. Theoretical vibrational analysis via Velocity Power Spectra (VPS)

The MD simulations can also be used to derive vibrational information. In particular, a velocity power spectrum (VPS) is determined by the Fourier transform of the velocities according to [13]:

$$I_{VPS}(\omega) = \lim_{t\to\infty} \frac{1}{t} \sum_{i=1}^{N} \sum_{\alpha=x,y,z} \left| \int_0^t v_{i,\alpha}(t) \mathrm{e}^{-\mathrm{i}\omega t}\, dt \right|^2$$

The VPS contains all vibrational frequencies and does not depend on any selection rules. It is related to the IR spectrum since this is the Fourier transform of the time derivative of the dipole moment $\mu_\alpha = \sum_i q_i R_{i\alpha}$.

$$I_{IR}(\omega) = \lim_{t\to\infty} \frac{1}{t} \sum_{\alpha=x,y,z} \left| \int_0^t \frac{d\mu_\alpha(t)}{dt} \mathrm{e}^{-\mathrm{i}\omega t}\, dt \right|^2$$

The main advantage is that the MD-derived VPS spectra account for the anharmonic effects, and hence go beyond the harmonic oscillator approximation usually adopted in a static normal mode analysis.

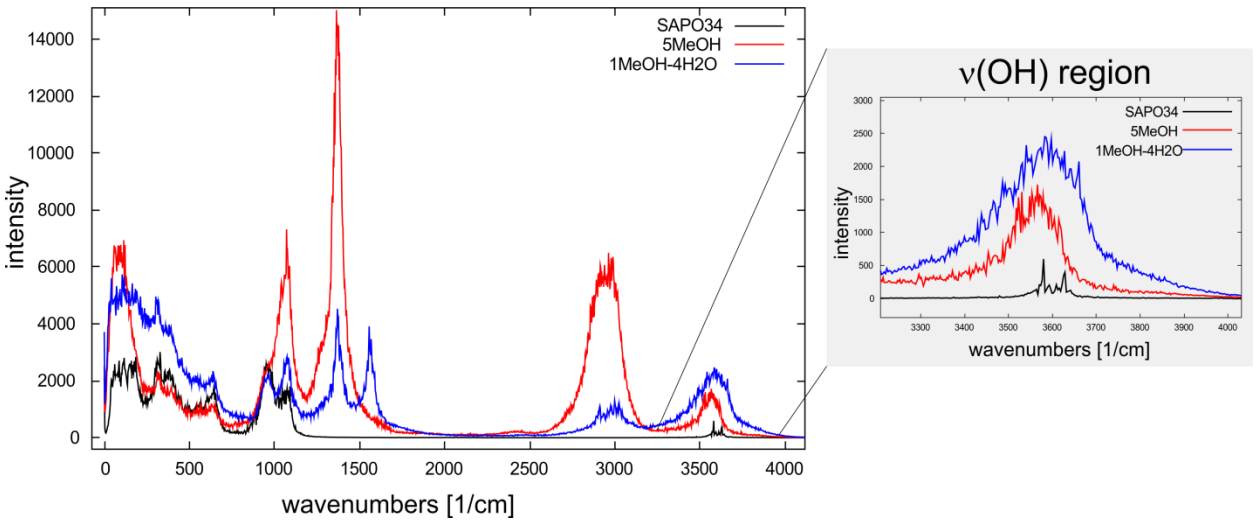

Figure S9. Theoretical VPS spectra of the parent SAPO-34 material (in black), compared with the results of SAPO-34 containing 5 MeOH molecules ($(5:0)_{mw,sim}$, in red) and 1MeOH-4H_2O molecules ($(1:4)_{mw,sim}$, in blue). All spectra are scaled to make sure that the stretching peak of the Brønsted acid site is centered at the experimental value of 3600 cm^{-1}.

Figure S9 displays the calculated VPS. The region corresponding with the OH stretch frequencies is particularly interesting as it shows the effect on the nature of the acid site of high methanol or water loadings. In the empty framework, two acid sites are present per unit cell. These acid sites are located in the same 8-ring and in the VPS give rise to two distinct peaks. When high loadings of protic molecules are adsorbed, the OH stretch region significantly broadens and this effect is more pronounced for water than for methanol. This observation indicates the presence of interactions between the hydrophilic framework and formation of water clusters.[14]

S5. Confocal fluorescence microscopy results

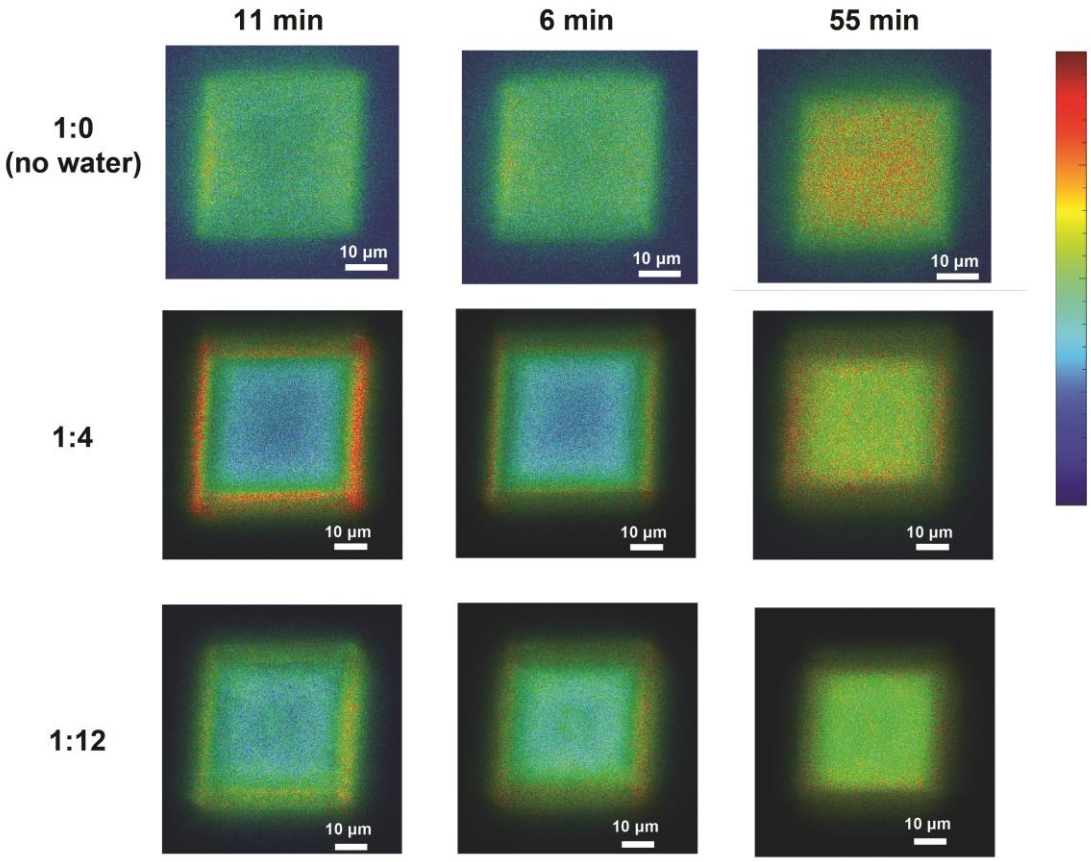

Figure S10. Confocal fluorescence microscopy images of single H-SAPO-34 crystals collected in-situ during MTO reaction at different water contents. The images were taken in the middle plane of the crystal and represent the red-to-green fluorescence ratio in color code.

S6. Catalyst steaming

Co-feeding the catalyst with water during the MTO reaction might cause the formation of mesopores, which could account for the more homogeneous formation of coke species throughout the whole SAPO-34 crystal. To evaluate the formation of mesopores, we steamed the SAPO-34 crystals at the reaction temperature (350 °C) in the same in-situ cell. Due to the low amount of sample during these experiments, we were unable to characterize these samples by N_2 physisorption measurements. As a result of these experimental limitations, we measured the formation of mesopores by adding a fluorescent dye, Nile Blue A (Figure S11a), which is only able to absorb in the mesopores of the material. The H-SAPO-34 crystals were first calcined in-situ for 1 hour at 500 °C under 50 ml/min O_2 flow and then steamed at 350 °C using N_2 as carrier gas. After the steaming process, approximately 15 ml of Nile Blue A were pipetted on fresh and steamed H-SAPO-34 samples. When the samples were dried the adsorption of Nile Blue was imaged by using confocal fluorescence microscopy with a 638 nm laser (diode laser, 150 mW). The confocal fluorescence microscopy images of the fresh and steamed SAPO-34 material were the same: no fluorescence inside of the crystals was observed and thus no mesopore formation. A representative picture of the top of the crystal is given in Figure S11b. These results are in line with other studies where typically temperatures of around 650 °C are needed to introduce mesopores in this type of materials.[15]

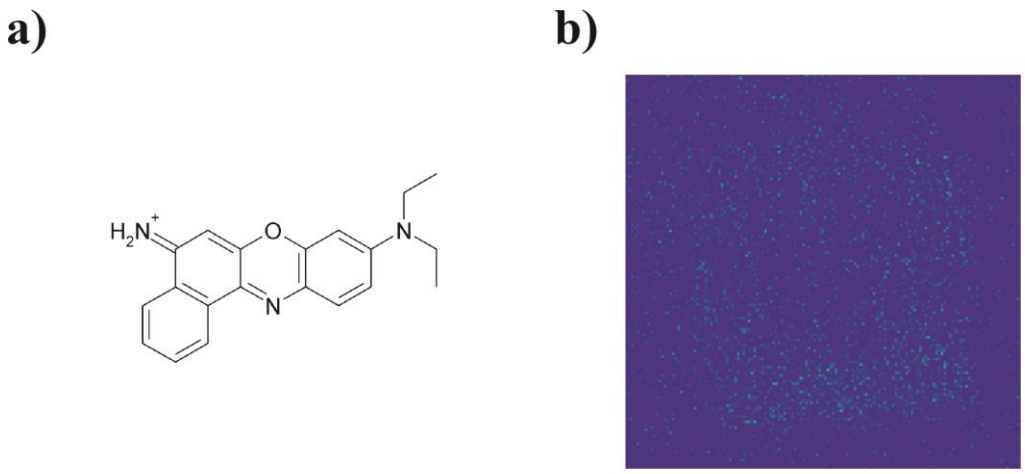

Figure S11. a) Molecular structure of Nile Blue A. b) Fluorescence micrograph of the top of a steamed H-SAPO-34 crystal treated with Nile Blue A.

References

(1) Ensing, B.; Laio, A.; Parrinello, M.; Klein, M. L. *J. Phys. Chem. B* **2005**, *109*, 6676-6759.

(2) Iannuzzi, M.; Laio, A.; Parrinello, M. *Phys. Rev. Lett.* **2003**, *90*, 4.

(3) Laio, A.; Gervasio, F. L. *Rep. Prog. Phys.* **2008**, *71*, 22.

(4) Laio, A.; Parrinello, M. *Proc. Natl. Acad. Sci. U. S. A.* **2002**, *99*, 12562-12566.

(5) Sutto, L.; Marsili, S.; Gervasio, F. L. *Wiley Interdiscip. Rev.: Comput. Mol. Sci.* **2012**, *2*, 771-779.

(6) De Wispelaere, K.; Ensing, B.; Ghysels, A.; Meijer, E. J.; Van Speybroeck, V. *Chem. Eur. J.* **2015**, *21*, 9385-9396.

(7) Moors, S. L. C.; De Wispelaere, K.; Van der Mynsbrugge, J.; Waroquier, M.; Van Speybroeck, V. *ACS Catal.* **2013**, *3*, 2556-2567.

(8) Westgård Erichsen, M.; De Wispelaere, K.; Hemelsoet, K.; Moors, S. L. C.; Deconinck, T.; Waroquier, M.; Svelle, S.; Van Speybroeck, V.; Olsbye, U. *J. Catal.* **2015**, *328*, 186-196.

(9) Van der Mynsbrugge, J.; Moors, S. L. C.; De Wispelaere, K.; Van Speybroeck, V. *ChemCatChem* **2014**, *6*, 1906-1918.

(10) Van Speybroeck, V.; De Wispelaere, K.; Van der Mynsbrugge, J.; Vandichel, M.; Hemelsoet, K.; Waroquier, M. *Chem. Soc. Rev.* **2014**, *43*, 7326-7357.

(11) ISP Optics, Janis research, http://www.janis.com/ (September 2015), Window Transmission Curves - Quartz SiO_2 Transmission Curce Data sheet.

(12) Marchi, A. J.; Froment, G. F. *Appl. Catal.* **1991**, *71*, 139-152.

(13) Van Houteghem, M.; Verstraelen, T.; Van Neck, D.; Kirschhock, C.; Martens, J. A.; Waroquier, M.; Van Speybroeck, V. *J. Chem. Theory Comput.* **2011**, *7*, 1045-1061.

(14) Okuhara, T. *Chem. Rev.* **2002**, *102*, 3641-3665.

(15) Aramburo, L. R.; Ruiz-Martínez, J.; Sommer, L.; Arstad, B.; Buitrago-Sierra, R.; Sepulveda-Escribano, A.; Zandbergen, H. W.; Olsbye, U.; de Groot, F. M. F.; Weckhuysen, B. M. *ChemCatChem* **2013**, *5*, 1386-1394.